PERGAMON

Journal of Structural Geology 21 (1999) 555–576

JOURNAL OF STRUCTURAL GEOLOGY

Nucleation of ductile shear zones in a granodiorite under greenschist facies conditions, Néouvielle massif, Pyrenees, France

Jacques Ingles[a,*], Christian Lamouroux[b], Jean-Claude Soula[c], Nicole Guerrero[d], Pierre Debat[a]

[a]*Laboratoire de Minéralogie, Université Paul Sabatier, 38, rue des Trente Six Ponts, 31400 Toulouse, France*
[b]*Laboratoire de Sédimentologie et de Géologie dynamique, Université des Sciences et Technologies de Lille, 59655 Villeneuve d'Asc Cedex, France*
[c]*Université Paul Sabatier, 38, rue des Trente Six Ponts, 31400 Toulouse, France*
[d]*ER 1746, Université Paul Sabatier, 38, rue des Trente Six Ponts, 31400 Toulouse, France*

Received 20 April 1998; accepted 27 January 1999

Abstract

The problem of ductile shear zone nucleation under greenschist facies conditions is approached from the example of small-scale shear zones developed in the Néouvielle granodioritic pluton (Pyrenees, France) by means of field and microstructural observations and chemical analyses. These shear zones are not related to pre-existing fractures and exhibit networks of numerous conjugate, fairly parallel and regularly spaced centimetre-scale brittle–ductile shear zones involving diffuse localization mechanisms.

Although the mode of deformation depends on the minerals present, deformation in the shear zones is basically controlled by hydration processes. Hydration and consequent fluid-controlled alteration and deformation are related to fluid migration towards developing cracks. All these cracks are extensional and formed on the scale of at most a few grains and frequently single grains. A comparison of chemical compositions of undeformed and sheared granodiorite shows that the shear zones can be interpreted as isochemical and isovolumetric systems.

We propose a sequence of mechanisms by which the nucleation of a small-scale brittle–ductile shear zones spreading out within a granodioritic rock may occur. In these mechanisms shear zone nucleation occurs independently of pre-existing fractures and results from the heterogeneous character of the polymineralic rock. In the studied granodiorite the mineral heterogeneities favour focusing of locally derived fluids by processes involving grain-scale hydraulic fracturing. Fluid focusing generates instabilities by local softening and subsequently shear zone nucleation.

1. Introduction

Nucleation and development of ductile shear zones is usually ascribed to local softening near the brittle–ductile transition. Softening is often related to fluid migration and infiltration towards or within the shear zones in geological settings ranging from large-scale open to grain-scale closed systems (Griggs and Blacic, 1964, 1965; Griggs, 1974; Beach, 1976; Kerrich et al., 1977; Brodie, 1981; Blacic and Christie, 1984; Etheridge et al., 1984; Kirby and Kronenberg, 1984; Gibson, 1990; Kronenberg et al., 1990; Oliver et al., 1990; Henderson and McCaig, 1996; Tullis et al., 1996; amongst others).

In the case of shear zones formed under greenschist facies metamorphic conditions, softening may be essentially related to hydraulic weakening (Griggs and Blacic, 1964, 1965; Raleigh and Paterson, 1965; Griggs, 1974; Kirby, 1984; Kronenberg et al., 1990; Tullis et al., 1996), grain boundary sliding and surface diffusion flow (Coble creep, Coble, 1963; Elliott, 1972; Kerrich et al., 1977, 1980; Kerrich, 1986) and/or mineral alteration and reaction softening (Mitra, 1978;

* Corresponding author.
E-mail address: geostruc@cict.fr (J. Ingles)

0191-8141/99/$ - see front matter
PII: S0191-8141(99)00042-5

White and Knipe, 1978; White et al., 1980; Gibson, 1990; Shea and Kronenberg, 1992, 1993; Mares and Kronenberg, 1993; O'Hara, 1994; Hickman et al., 1995; Wintsch et al., 1995). Softening mechanisms not related to fluid effects such as dislocation creep or dynamic recrystallization (Vidal et al., 1980; Knipe, 1989) seem less common or less efficient. In polymineralic rocks, alteration of strong mineral phases, such as feldspars in granodiorite, can be the most efficient softening mechanism (Hippertt, 1998).

Two modes of nucleation and development of ductile shear zones have been invoked depending on whether the shear zones develop along pre-existing fractures (Rudnicki, 1977; Segall and Pollard, 1983; Segall and Simpson, 1986; Gibson, 1990; Kronenberg et al., 1990; Tourigny and Tremblay, 1997) or are unrelated to pre-existing fractures and propagated as banded structures from discrete nucleation sites (Cobbold, 1977; Poirier, 1980; White et al., 1980).

In the former case, softening results from fluid infiltration along open transgranular cracks. Kronenberg et al. (1990) suggested that water related defects gained access to grain interiors and dislocation cores by pipe diffusion along mobile dislocations following fluid infiltration. It is implicit in this case that nucleation (and development) of shear zones will be controlled by the presence of pre-existing fractures, their orientation and the ability of fluids to focus into them.

In the latter case, nucleation and development of ductile shear are zones proceeded by plastic deformation of 'soft' minerals which allow the 'hard' minerals (if present) to be re-oriented as rigid particles in a ductile matrix. In granitic rocks, in greenschist facies conditions, quartz is the only essential mineral which deforms by plastic deformation. However, its content ($<30\%$) is not sufficient for the other ('hard') grains to rotate in order to accommodate large finite strains as recorded in ductile shear zones (Gay, 1968; Debat et al., 1975, 1978; Handy, 1990, 1994). In this case, a shear zone will nucleate only if a sufficient quantity of 'hard' minerals soften before and during deformation. Fluids responsible for grain softening will circulate towards grain-scale open discontinuities such as intragranular, intergranular or transgranular fractures (Cox and Etheridge, 1989) via grain boundaries or transgranular discontinuity surfaces.

The problem of ductile shear zone nucleation is approached here from the example of small-scale shear zones not related to fractures or veins, occurring in the Néouvielle granodioritic pluton. Because of their small dimensions, structural as well as mineralogical or chemical changes may be thouroughly followed. Moreover, the relatively small value of finite strain they record enables us to investigate the earliest deformational stages more conveniently than higher strain and larger shear zones.

2. Geological setting

The Néouvielle massif is a Hercynian synkinematic granodiorite emplaced into low grade metasedimentory rocks of the Axial Zone of the Central Pyrenees (Lamouroux, 1976, 1987; Pouget et al., 1989).

This massif is affected by two types of Alpine shear zones (Fig. 1) (Lamouroux, 1976, 1987; Lamouroux et al., 1979, 1980, 1991; Soula et al., 1986): (i) regional shear zones having thickness of tens of metres across the tens of kilometres of lateral exposure; (ii) small-scale shear zones with thickness of tens of centimetres across the few metres of lateral exposure.

2.1. Regional shear zones

In the Néouvielle massif 14 regional shear zones trending N110°E have been recognized and first studied by Lamouroux (1976, 1987). One of them, the Pic Long shear zone, which is situated close to the southern contact between the granodiorite and Devonian metasediments (Fig. 1) has been analysed in detail by Losh (1989) and Henderson and McCaig (1996).

These shear zones pass beyond the contact between granodiorite and country rocks and display small dextral horizontal displacement (tens of metres). In vertical sections perpendicular to their trend they define a fan-shaped structural pattern with vertical reverse displacements.

The regional shear zones show various structural characteristics: (1) they consist of distinct rock types developing as a function of increasing strain: unsheared granodiorite, protomylonite, mylonite, ultramylonite, phyllonite (Lamouroux, 1976, 1987; Losh, 1989); (2) they are associated with brittle faults displaying reverse or normal movements which crosscut the ductile mylonitic structures (Henderson and McCaig, 1996); (3) they contain numerous veins filled with quartz, chlorite, calcite and actinolite (Henderson and McCaig, 1996).

2.2. Small-scale shear zones

Small-scale shear zones are well developed in the central and southern parts of the massif. In the previously unmylonitized material, they define networks formed by two conjugate sets (Fig. 2a, b) both trending N100°E. Set 1 dips 30° towards the north and set 2 dips 45° towards the south (Lamouroux et al., 1991, 1994, fig. 3). Their internal structures (foliation trajectories, tension gashes and grain rotation) indicate opposite displacement senses for the two conjugate sets which gives rise to almost symmetrical offsets. The principal finite shortening direction bisects the acute angle made by the two sets (Lamouroux et al., 1991,

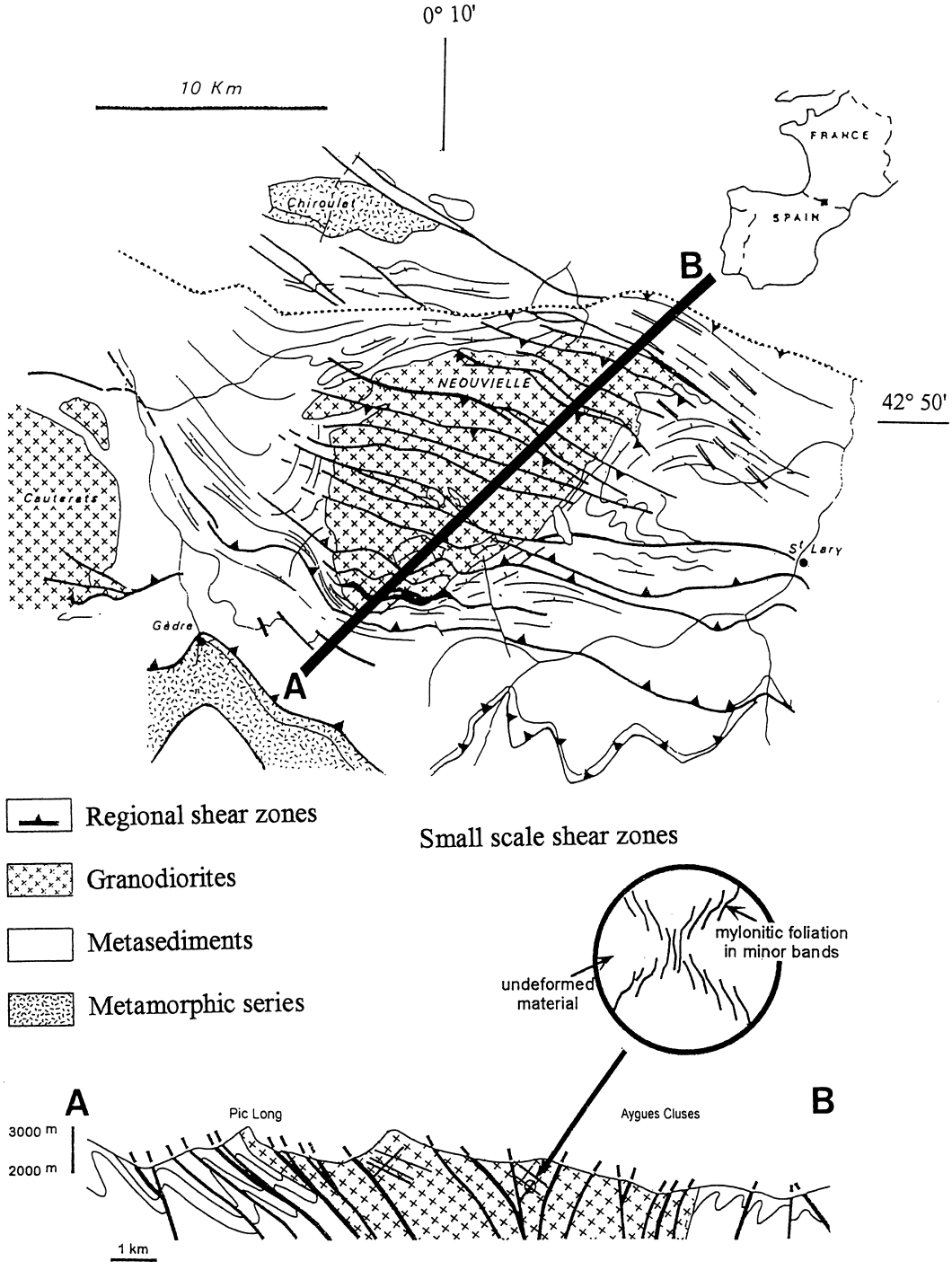

Fig. 1. Néouvielle massif: schematic map and cross-section (AB); location of the small scale shear zones.

1994) and is north–south and horizontal (Fig. 2a). In contrast with the regional-scale shear zones, the small-scale shear zones are neither cross-cut by, nor related to, brittle faults.

All the shear zones are Alpine in age (Lamouroux et al., 1979, 1980, 1981). Radiometric dating of the regional shear zones gave an age of 48 Ma (Wayne and McCaig, 1998).

3. Characteristics of the small-scale shear zones

The small-scale shear zones form within an undeformed granodiorite composed of $<30\%$ quartz, 40% plagioclase, 10% perthitic microcline, 15% biotite and 5% amphibole + allanite. The grains have an average dimension of 1–2 cm and contain no deformation structures except occasional undulose extinction in

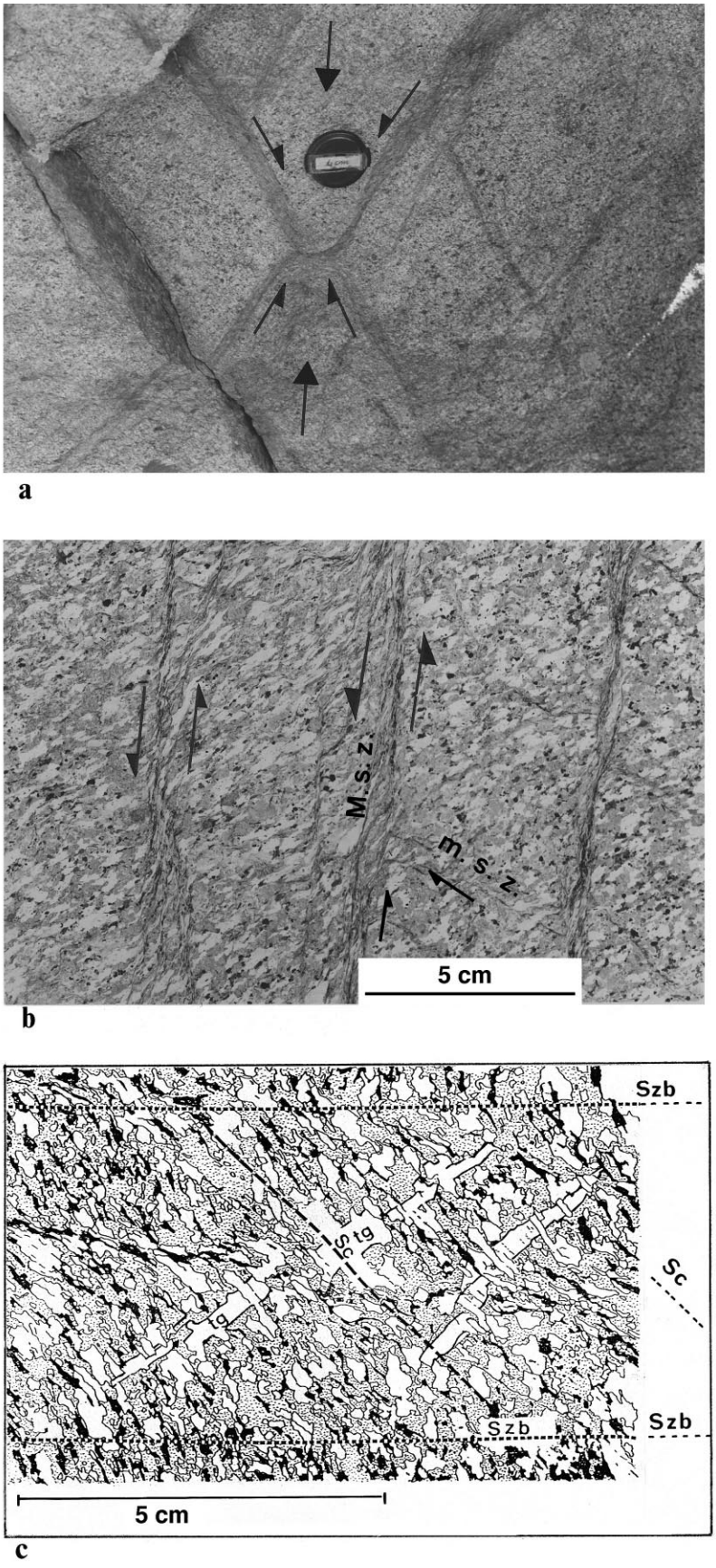

Fig. 2. (a) Network of conjugate small-scale shear zones. (b) Small-scale shear zones. The shear zones appear as regularly spaced very high strain zones within less strained regions. One of the conjugate sets is here largely prominent. M.s.z: major shear zone set; m.s.z: minor shear zone set. (c) Moderate strain shear zone showing a sigmoidal trajectory of the foliation (Sc). Szb: shear zone boundary; tg: tension gash.

quartz. This granodiorite lacks any original magmatic foliation. At outcrop scale, it can be considered as a homogeneous and isotropic material. The small-scale shear zones are lenticular, 2–10 cm thick and 1–5 m long and wide, with flat planar boundaries at sample scale. Depending upon the amount of finite strain accommodated by the entire shear zones, two types of internal structures may be distinguished.

3.1. Moderate strain shear zones

In these shear zones, the internal foliation outlined by biotite and amphibole flakes and quartz aggregates, has an almost symmetrical sigmoidal trajectory with an inflexion line lying in the median part of the zone (Fig. 2c). The maximum shear strain (γ_{max}) as estimated from the geometry of the foliation trajectory (Ramsay and Graham, 1970; Ramsay and Huber, 1987) varies from 2.6 to 4.5 and the corresponding maximum extension (e_1) from 200 to 370% (Lamouroux et al., 1994, fig. 7). Within the zone, the increase in strain is associated with changes in grain dimension and shape, as usually seen in shear zones. Their elongation (length–width ratio) varies from less than 2 near the shear zone boundary, to 4 in its median part (Lamouroux et al., 1994). Biotite (Fig. 3a), amphibole (Fig. 3b) and allanite (Fig. 3c, d) show pinch and swell structures with more or less elongate necks which formed from the altered parts of the minerals. Necking is accompanied by pulling apart parallel to the foliation or block rotation ('domino' structures) of the non- or less altered parts of these minerals (Fig. 3b). With increasing strain, the necked crystals evolve into separate grains with individual tails. Feldspars are

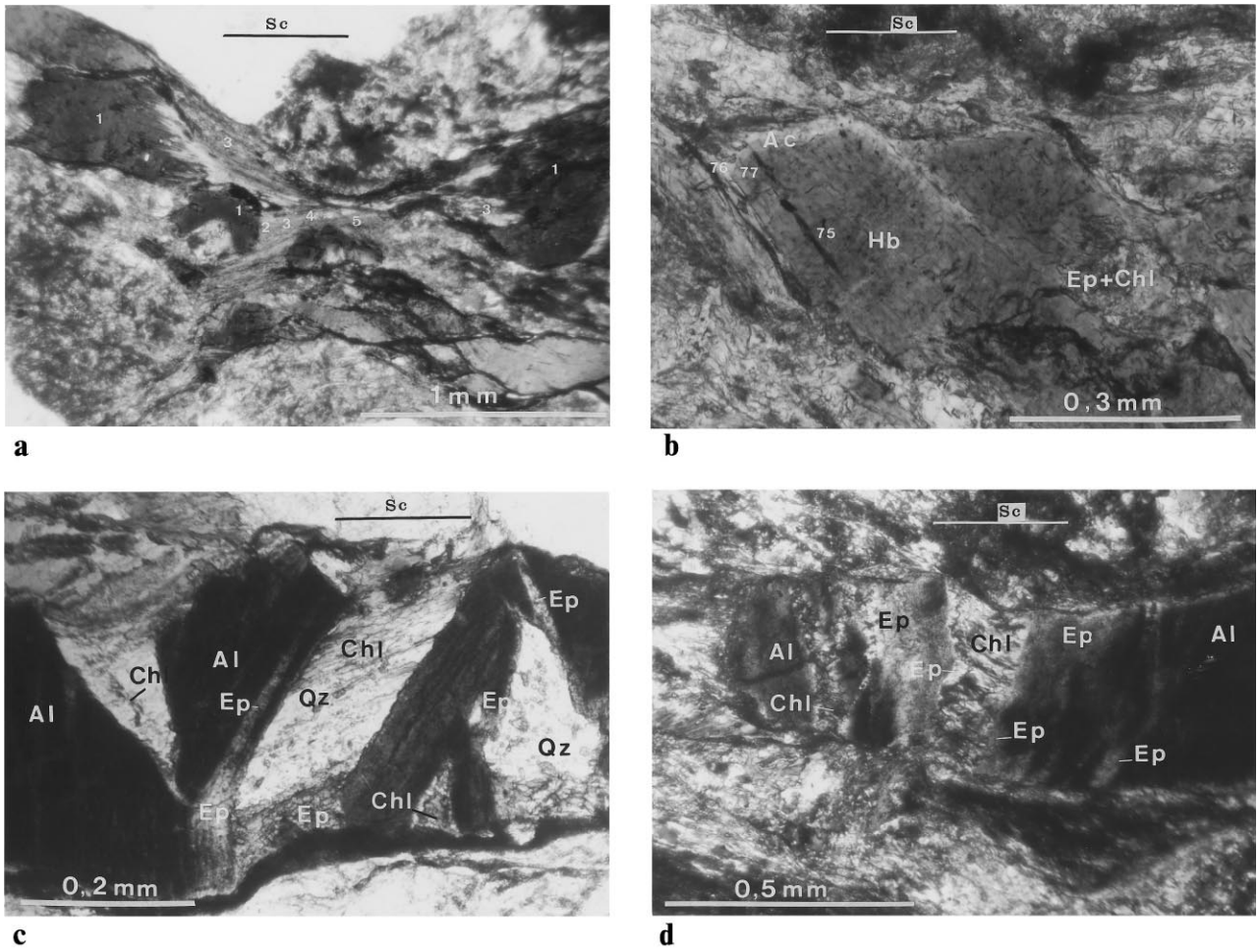

Fig. 3. (a) Pinch and swell structure in biotite with chloritized biotite tails developing from the tips of the grains. 1, 2, 3, 4, 5 refer to Bi1, Bi2, Bi3, Bi4 and Bi5 in Figs. 9 and 10 and in Table 3. (b) Domino structure in amphibole. Hornblende blocks are rimmed by actinolite. 75, 76, 77 refer to analyses plotted in Fig. 8 and given in Table 3. Hb: hornblende; Ac: actinolite. (c) Brittle failure with block separation in allanite, the intergranular spaces being filled with epidote + chlorite and/or quartz + chlorite intergrowths. Al: allanite; Ep: epidote; Chl: chlorite; Qz: quartz. (d) Necking related to alteration in allanite. The neck formed in the thickest of the alteration bands consisting of epidote and/or epidote + chlorite which developed across the entire width of the grain (see details in Fig. 6).

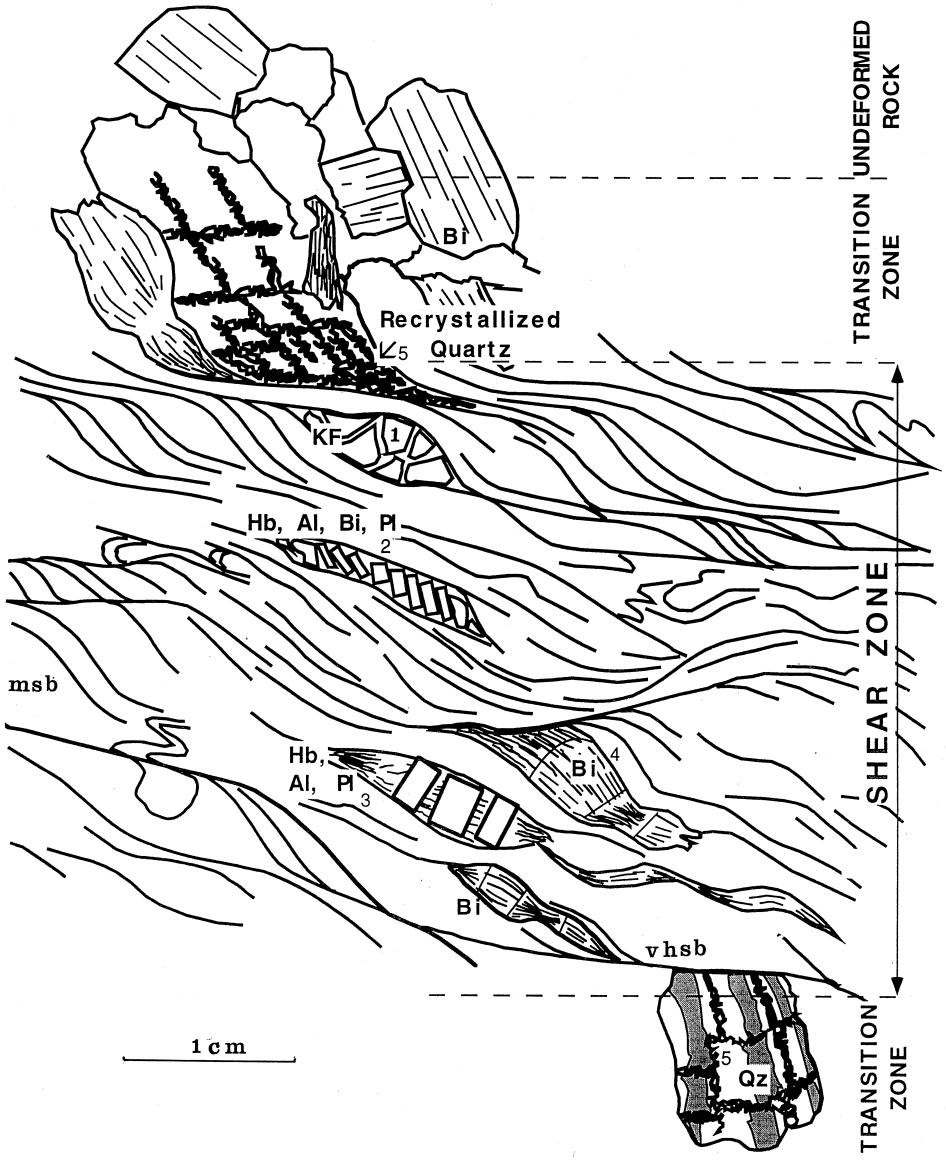

Fig. 4. Diagrammatic section of a high strain shear zone showing the various types of deformation structures. This high strain shear zone is composed of moderate to high strain bands (msb) showing a sigmoidal trajectory of the foliation, separated by thin very high strain bands (vhsb) parallel to the shear zone wall. 1: Open conjugate fractures; 2: domino structures; 3: untilted pulled apart blocks; 4: pinch and swell structures. Qz: quartz; Al: allanite; Bi: biotite; Hb: hornblende; KF: K-feldspar; Pl: plagioclase.

only affected by internal open conjugate fractures. These structures give rise to untilted pulled-apart blocks or dominoes (Fig. 4).

In addition to grain-scale extension fissures, veins which are several grains long ('transgranular' microfractures, according to Cox and Etheridge, 1989) may develop perpendicular to the foliation.

3.2. High strain shear zones

Their internal structure is markedly heterogeneous with moderate to high strain bands (msb) where the foliation shows a sigmoidal trajectory, separated by thin dark-coloured very high strain bands (vhsb) parallel to the shear zone wall, where the microstructures are indiscernible (Fig. 4). In the very high strain bands, microprobe analyses show that epidote, chlorite and quartz are present. Within the moderate to high strain bands, the microstructures are roughly similar to those found in the moderate strain shear zones except for quartz and feldspars. Quartz appears as σ-shaped polycrystalline aggregates parallel to the foliation with coarser grains rimmed by smaller polygonal grains which can be considered as diagnostic of dynamic recrystallization (Hobbs, 1968; Bell and Etheridge, 1976; White, 1977; Lamouroux, 1987; amongst others).

Feldspars are more altered and smaller than in the moderate strain shear zones but they keep their euhedral shape.

The sigmoidal foliation of the moderate to high strain bands may pass progressively into the very high strain bands, the bands thus appearing as classical '*C–S* structures' (Berthé et al., 1979; Ramsay and Huber, 1987). More frequently, however, the very high strain bands cross-cut the foliation of the moderate to high strain bands and appear as discontinuity planes (Fig. 4).

4. Alteration and deformation within the shear zones

4.1. Minerals

As frequently oberved in shear zones formed under greenschist facies metamorphic conditions, alteration essentially results from hydration reactions. Although the mode of deformation depends on the crystal species, finite strain is a function of the state of alteration in all minerals.

Plagioclase which has an average composition of An_{40} (Table 1, Fig. 5) and a normal zonation (An_{53} in the core and An_{30} in the rim) in the undeformed rock is affected by saussuritization in the shear zone. This process alters the plagioclase with development of epidote, chlorite and calcite and produces an overall albitization of the crystal as pointed out by Kamineni et al. (1988) amongst others. This process requires a fluid supply (Nutman et al., 1989; Wintsch et al., 1995), essentially H_2O and CO_2, and releases Ca and SiO_2. The chlorite, epidote and calcite grains are localized within intragranular open fractures and extension fissures or occur in contact with the faces of the grain perpendicular to the foliation. Where the plagioclases are the most altered, the intragranular extension fissures are wide and the grains are separated into pulled apart blocks often rotated as 'dominoes'. In this case, the inter-block spaces filled with alteration products (chlorite, epidote, ±calcite) and quartz are necked but the feldspar blocks preserve their idiomorphic shape whatever their alteration state. The length–width ratio of the grains parallel to the foliation increases with increasing strain. This strongly suggests that the alteration products were dissolved on the face perpendicular to the shortening direction and transported by, and/or migrated within, fluids. This explains why the plagioclase grains preserved their brittle behaviour and their competency during the entire deformational process. This suggests also that plagioclase deformed as a result of pressure-solution. Cross-cutting of plagioclase grains by the very high strain bands with sharp indented boundaries gives evidence that plagioclase was sensitive to pressure-solution. K-feldspar alteration results in the formation of albite, quartz and less frequently sericite (K-rich white micas) infilling intragranular open fractures. The deformational behaviour of K-feldspar crystals appears to have been similar to that of plagioclase.

The alteration and alteration-controlled deformation processes differ markedly in ferromagnesian minerals. There, alteration progressing towards the interiors of the grains essentially proceeded as a solid state transformation inducing a progressive softening of these grains. This may be achieved either by solid-state diffusion or, more probably, by fluids penetrating the grain interiors via interconnected microcracks.

Allanite (Table 2) is rather rare but shows characteristic alteration features which can be taken as a reference for interpretating the alteration features in the other ferromagnesian minerals. Allanite grains show two modes of deformation: (1) brittle failure with separation of blocks accompanied by a weak alteration limited to the faces of the grains (Fig. 3c); (2) necking related to a well marked alteration of the entire width of the grain (Fig. 3d).

In the case of brittle failure, the intergranular spaces are filled with quartz + chlorite intergrowths and/or epidote (Table 1). Quartz + chlorite intergrowths are likely to result from the deposition of fluid-transported minerals. Epidote probably originates, at least partly, from the altered face of the allanite. The infilling features (Fig. 3c) are here similar to those resulting from crack-sealing mechanisms (antitaxial and composite modes, according to Ramsay and Huber, 1987).

In the case of necking, alteration appears as bands with a characteristic zoning developing across the entire width of the crystals (Figs. 3d and 6). The external zone is composed of a network of unaltered allanite with interstitial epidote small grains, the intermediate zone is composed of epidote small grains with rare remnants of the host grain, and the central zone is composed of chlorite. Such a complete zoning is observed only in the most altered bands. There, the chlorite zone may attain a thickness of the same order of magnitude as the width of the grain (Figs. 3d and 6). In less altered parts of the crystal, only epidote appears in the central zone. Allanite + epidote bands or patches alone are observed where alteration is weak. In the most altered parts of the grain, not only the chlorite but also the epidote and the epidote + allanite bands, are thicker than in the less altered parts of the grain (Figs. 3d and 6). The alteration features may also be reduced to epidote-rimmed chlorite wedges extending into epidote + allanite bands (Figs. 3d and 6). These features strongly suggest that alteration resulted from progressive fluid (H_2O, SiO_2) infiltration through deformation-induced open cracks (Fig. 7). According to Parseval (1992), the transformation epidote → chlorite is achieved by dissolution of epidote

Table 1
Plagioclase, epidote and chlorite analyses

Sample	Undeformed rock		Shear zone		Shear zone			Shear zone			
Mineral	Plagioclase		Plagioclase		Epidote	Epidote	Epidote	Chlorite	Chlorite	Chlorite	Chlorite
Remarks	Core	Rim	Core	Rim	Associated with allanite	Associated with plagio	Within veins	Associated with biotite	Associated with allanite	Within veins	Ass. with recrystall. quartz
	av. of 6 analyses	av. of 6 analyses	av. of 6 analyses	av. of 5 analyses	av. of 3 analyses	av. of 2 analyses	av. of 5 analyses	av. of 3 analyses	av. of 2 analyses	av. of 3 analyses	av. of 2 analyses
SiO_2	54.71	58.01	56.29	67.03	37.49	36.31	37.22	24.59	24.60	25.14	25.47
TiO_2	0.00	0.03	0.00	0.08	0.00	0.03	0.12	0.02	0.03	0.00	0.03
Al_2O_3	26.62	26.50	24.56	19.52	26.86	27.38	27.17	19.10	18.88	18.28	19.53
FeO	0.12	0.06	0.13	0.06	7.05	5.04	6.09	28.95	28.91	27.92	26.23
MnO	0.00	0.00	0.00	0.00	0.00	0.00	0.00	0.45	0.56	0.56	0.53
MgO	0.00	0.00	0.00	0.00	0.43	0.03	0.01	11.96	11.66	12.42	11.70
CaO	11.08	8.83	8.71	0.65	22.71	23.77	24.01	0.00	0.00	0.00	0.00
Na_2O	5.43	6.66	6.74	11.07	0.01	0.02	0.03	0.04	0.05	0.06	0.04
K_2O	0.09	0.22	0.06	0.43	0.23	0.00	0.03	0.02	0.05	0.00	0.36
Total	98.04	99.87	96.48	98.83	94.78	92.58	94.69	85.12	84.72	84.38	83.87
Structural formulae on a basis of 8 oxygens for plagioclases, on the basis of 12.5 for epidotes and on the basis of 28 for chlorites											
Si	2.52	2.59	2.62	2.97	2.97	2.93	2.96	5.49	5.52	5.63	5.68
Al	1.35	1.45	1.13	1.07	2.50	2.61	2.56	5.02	5.50	4.83	5.13
Ti	0.00	0.00	0.00	0.00	0.00	0.00	0.01	0.00	0.00	0.00	0.01
Fe	0.00	0.00	0.00	0.00	0.47	0.34	0.41	5.40	5.43	5.23	4.89
Mn	0.00	0.00	0.00	0.00	0.00	0.00	0.00	0.08	0.11	0.11	0.10
Mg	0.00	0.00	0.00	0.00	0.05	0.00	0.00	3.98	3.90	4.15	3.89
Ca	0.55	0.42	0.43	0.03	2.28	2.37	2.32	0.00	0.00	0.00	0.00
Na	0.48	0.58	0.61	0.95	0.00	0.00	0.00	0.02	0.02	0.03	0.02
K	0.01	0.01	0.00	0.02	0.02	0.00	0.00	0.01	0.01	0.00	0.10

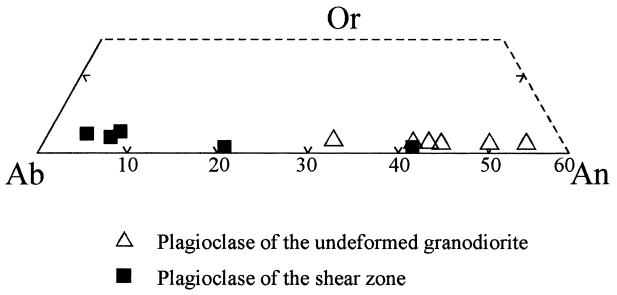

Fig. 5. Composition of plagioclases in the Or–Ab–An diagram.

and redeposition of chlorite. The crystallization mechanism of chlorite is, in this respect, similar to usual crack–seal mechanisms (Ramsay and Huber, 1987). The progression of alteration towards the interiors of the grains suggests a progressive epidotization of the allanite as a result of fluid infiltration via open cracks. This is followed by the dissolution of the crack wall epidote and consequent deposition of chlorite within the crack, at the same time as fluid penetrating more deeply within the grain caused epidotization of previously non-altered parts of this grain (Fig. 7). Necking is localized in the most altered parts of the grains, comprising the chlorite zone and a small part of the epidote zone.

In both cases (block separation or necking), alteration appears to have developed from microcracks scattered within the grain which allowed the fluids to penetrate the grain interiors. In the former case, the microcracks propagate along the entire width of the grains and open in the earlier stages of the process. In the latter stage, fluids penetrate more deeply into the grain interiors before opening and ductile deformation can occur.

Amphibole crystals observed within the shear zones appear as small tilted and/or pulled apart blocks arranged as 'domino structures' (Fig. 3b) similar to those previously described by Allison and La Tour (1977), Babaie and La Tour (1994) and Takagi (1989). These blocks are zoned with a dark-green core of hornblende and a pale-green rim of actinolite (Figs. 3b and 8 and Table 3). In the less evolved structures, the actinolite rim is common to two adjacent dominoes and constitutes the slip zone between them. This suggests that a deformation-induced and fluid infilled crack enhanced the hornblende→actinolite transformation. These amphibole grains are usually altered into epidote and chlorite. Epidote is essentially observed at the edges of the blocks (Fig. 3b). Chlorite is essentially found in the inter-block spaces and within intragranular cracks. These alteration features are responsible for the overall 'pinch and swell' appearance of the amphiboles.

Biotite alteration results in the pseudomorphic trans-

Table 2
Allanite analyses

Sample	Shear zone All-1	All-2
F_2O	0.484	0
MgO	0.70	0.73
Al_2O_3	16.87	16.06
SiO_2	31.59	30.71
Y_2O_3	0.222	0.175
Nd_2O_3	4.084	3.884
Pr_2O_3	0.824	0.814
Ce_2O_3	9.508	10.255
La_2O_3	5.272	5.404
TiO_2	0.62	0.59
CaO	12.37	11.88
ThO_2	1.705	1.686
Gd_2O_3	0.266	0.036
Dy_2O_3	0	0
Fe_2O_3	12.82	12.96
Sm_2O_3	0.645	0
Total	74.96	72.93

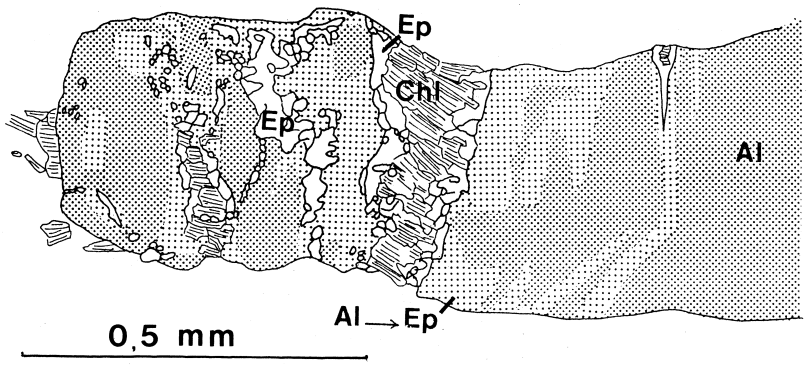

Fig. 6. Alteration features resulting from progressive fluid infiltration through deformation-induced open cracks in allanite (Al). Alteration zones are composed of epidote (Ep) and epidote + chlorite (Chl). The areas where the transformation of allanite into epidote is incomplete are indicated by a lighter ornament (Al→Ep). Note that the thickest alteration band where the neck formed is surrounded by the widest (Al→Ep) area. The right part of the grain is weakly altered and only a thin chlorite + epidote wedge is observed in the upper side.

Table 3
Amphibole and phyllosilicate analyses. Note that the analysed chlorites have the same composition whatever the mineral assemblage. A1 is an average of five analyses of amphibole from the undeformed granodiorite. A2 and A3 are averages of six analyses from the core of amphibole from the sheared granodiorite. A4 is an average of seven analyses from the rim of amphibole from the sheared granodiorite. Bi0 is an average of five analyses in the undeformed granodiorite. Bi1 is an average of five analyses in the core of a biotite from the sheared granodiorite. Bi2, Bi3, Bi4, Bi5 are phyllites from the tail of the same biotite grain and refer to 1, 2, 3, 4, 5 in Fig. 3(a). Bia is an average of four analyses from the tail of four different sheared biotite grains

Sample	Undeformed rock	Shear zone			Undeformed rock	Shear zone						
Mineral	Amph.	Amph. Core	Amph. Core	Amph. Rim	Biotite	Biotite Core	Biotite Tail	Biotite Tail	Biotite Tail	Biotite Tail	Biotite Tail	Chlorite
Remarks	A1	A2	A3	A4	Bi0	Bi1	Bi2	Bi3	Bi4	Bi5	Bia	Chl
SiO_2	48.71	46.99	48.52	51.74	36.30	36.19	35.3	34.2	31.5	29.1	29.1	25.66
TiO_2	0.55	0.71	0.55	0.06	2.83	3.37	0.24	0.39	0.23	0.04	0.14	0.00
Al_2O_3	5.23	6.26	5.71	2.91	14.30	14.27	16.3	17.22	18.46	19.6	18.8	19.64
FeO	16.86	18.93	18.44	16.51	21.13	22.33	20.9	21.78	25.06	26.9	26.8	28.25
MnO	0.46	0.58	0.43	0.36	0.25	0.28	0.34	0.38	0.36	0.53	0.59	0.54
MgO	11.06	9.27	9.80	11.84	9.96	8.76	10.4	10.5	11.56	11.8	11.8	12.49
CaO	10.93	10.94	11.64	12.16	0.06	0.01	0.21	0.04	0.12	0	0	0.06
Na_2O	0.92	0.97	0.84	0.34	0.15	0	0.03	0	0.07	0.05	0.07	0.03
K_2O	0.53	0.58	0.49	0.24	9.26	9.45	7.82	7.72	4.6	2.31	2.42	0.06
Total	95.25	95.21	96.41	96.16	94.25	94.66	91.54	92.23	91.96	90.33	89.72	86.72
Structural formulae on the basis of 23 oxygens for amphiboles, on the basis of 22 for the biotites and the basis of 28 for the chlorite												
Si	7.34	7.18	7.33	7.73	5.66	5.66	5.62	5.43	5.04	6.04	6.09	5.57
Al^{IV}	0.66	0.82	0.67	0.27	2.34	2.34	2.38	2.57	2.96	1.96	1.91	2.43
Al^{VI}	0.27	0.31	0.35	0.25	0.29	0.29	0.67	0.65	0.51	2.83	2.73	2.61
Ti	0.06	0.08	0.06	0.01	0.33	0.40	0.03	0.05	0.03	0.01	0.02	0.00
Fe^{+3}	0.33	0.32	0.08	0.06	2.76	2.92	2.78	2.89	3.35	4.67	4.69	5.13
Fe^{+2}	1.79	2.10	2.25	2.01								
Mn	0.06	0.08	0.05	0.05	0.03	0.04	0.05	0.05	0.05	0.09	0.10	0.10
Mg	2.48	2.11	2.21	2.64	2.32	2.04	2.47	2.48	2.75	3.65	3.68	4.04
Ca	1.78	1.81	1.89	1.95	0.01	0.00	0.04	0.01	0.02	0.00	0.00	0.01
Na	0.27	0.29	0.25	0.10	0.04	0.00	0.01	0.00	0.02	0.02	0.03	0.01
K	0.10	0.11	0.10	0.05	1.84	1.89	1.59	1.56	0.94	0.61	0.65	0.02

formation of the original crystal into an intergrowth of highly chloritized biotite and quartz (Fig. 3a and Table 3). The altered parts of the grains form the necks in the 'pinch and swell' structures and tails at the tips of individual grains. From the unaltered to the most altered part of the grain, the composition of the phyllosilicate evolves (Fig. 9) with a regular decrease in SiO_2 and K_2O, and increase in MgO, FeO and Al_2O_3 (Fig. 10 and Table 3). Finite strain is a function of this state of alteration and the most altered parts of the grains form very elongate necks or tails whereas less altered zones are less deformed. Microscopic observation indicates that the basal plane (001) of the chloritized biotite is in continuity with that of the host biotite. This shows that alteration proceeded here as a solid state transformation which converts biotite, which is otherwise rather strong and rigid when compressed perpendicular to (001), into a ductile and much softer pseudomorph. In the same manner as in allanite and amphibole, the alteration process is thought to have been triggered by the formation of microcracks allowing the penetration of fluids into the grain.

4.2. Veins

On the whole, intra-shear zone veins appear as en échelon sigmoidal extension fissures perpendicular to the foliation which are observed only in the moderate strain shear zones (Fig. 2c). These are few in number and their volume does not exceed 7% of the volume of the shear zone where they are the most numerous. Nevertheless, the geometry of the vein walls and the characteristics of the mineral infill appear to be significant in terms of the mode of nucleation of the shear zone. Although they seem, at first sight, to form continuous veins across the entire shear zone width, a closer examination shows that they are composed of more or less aligned individual short veins, 3–5 minerals long, separated from one another by elongate quartz grains or biotite flakes (Figs. 2c and 11a–c). The sense of apparent offset is either right-lateral or

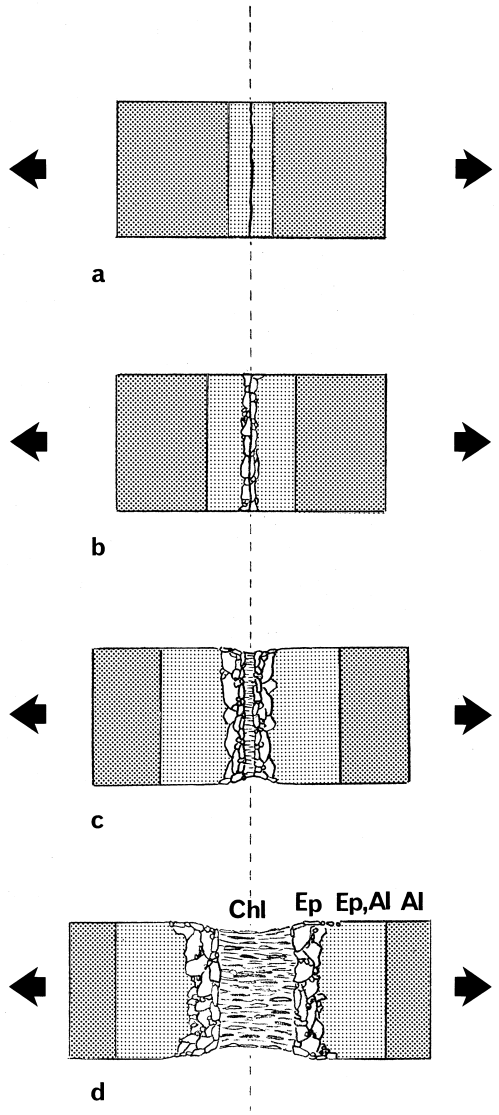

Fig. 7. Progression of alteration resulting from progressive fluid infiltration through deformation-induced open cracks. (a) Fluids penetrate into the crystal through open cracks and transform allanite incompletely into epidote (epidote + allanite areas). (b) Epidote alone forms in the crack wall while the transformation allanite → epidote progresses deeper within the grain. (c), (d) Chlorite, resulting from solution of crack wall epidote crystallizes from fluids infilling the open crack while the allanite → epidote, transformation progresses still deeper within the grain.

left-lateral and the vein thickness may vary markedly from one vein to another. Within each of these individual veins, the vein walls are discontinuous and are well defined only where the mineral in the wall rock is K-feldspar or plagioclase. As frequently observed in crack–seal structures, the infilling minerals are 'compositionally related to the crystals found in the wall rock' (Ramsay and Huber, 1987, p. 576). However, crack–seal features as described by, e.g. Ramsay and Huber (1987) are found only in contact with plagioclases and to a lesser extent K-feldspar. There, chlorite + epidote + quartz + calcite are seen growing from the plagioclase crystal (Fig. 11b). Calcite and epidote have no preferred orientation. Chlorite is perpendicular to the vein wall and parallel to the rock foliation. Where quartz crystallizes in contact with plagioclase, it contains the usual inclusion bands parallel to the vein walls (Fig. 11c, d). No such inclusion bands are found within the quartz grains deposited in more internal parts of the veins.

In contact with K-feldspar, there are sericite (K-rich white micas), albite and quartz (Fig. 11c). No preferred orientation or inclusion bands are observed.

In contact with biotite, one can observe either 'pure' chlorite (Fig. 11b) or chloritized biotite (Fig. 11e, f). 'Pure' chlorite (0% K_2O) (Table 3) is observed where the vein wall is constituted by a face of an unaltered biotite crystal. The chlorite aggregates are not necked and the chlorite flakes show a preferred orientation parallel to the rock foliation (Fig. 11b). This is interpreted as a result of deposition from fluids. Chloritized biotite ($K_2O > 2\%$) is observed associated with quartz where a biotite grain is traversed by the vein (Fig. 11e, f). It appears as an alteration feature similar to those observed in biotite outside the vein. In the same manner as in the wall rock, the chloritized biotite pseudomorphs are necked and contain inclusions of unaltered or less altered biotite (Fig. 11e, f). There, the boundary between vein and wall rock is diffuse and the development of chloritized biotite must be interpreted as a result of solid-state alteration in the wall rock, rather than of deposition from fluids. Alteration and consequent finite strain seem, however, greater than in the wall rock, as shown by the greater elongation of the necks. 'Vein' widening resulted here from propagation of alteration, i.e. penetration of fluids, within the grain through strain-induced microcracks and consequent ductile deformation.

The behaviour of quartz in the veins is especially interesting because the quartz grains of the wall rock often prolongate into or across the vein and/or constitute its upper and lower boundaries. The quartz grains in the vein appear to be more elongate than in the wall rock (Fig. 2c): near the median line of the shear zones, the axial ratios are from 6:1 to 9:1 in the vein instead of from 4:1 to 7:1 in the wall rock. These quartz grains display neither the multiple inclusion bands and trails which are observed in the quartz formed in contact with plagioclase nor the trace of the old grain boundaries found in the grains lengthened by pressure-solution–redeposition processes (Elliott, 1972). The elongation of the grains is likely to have been due to fluid-enhanced ductile deformation with, at most, a limited amount of additional deposition from circulating fluids.

On the whole, it appears that deformation, alteration and crack–seal mechanisms are the same in the

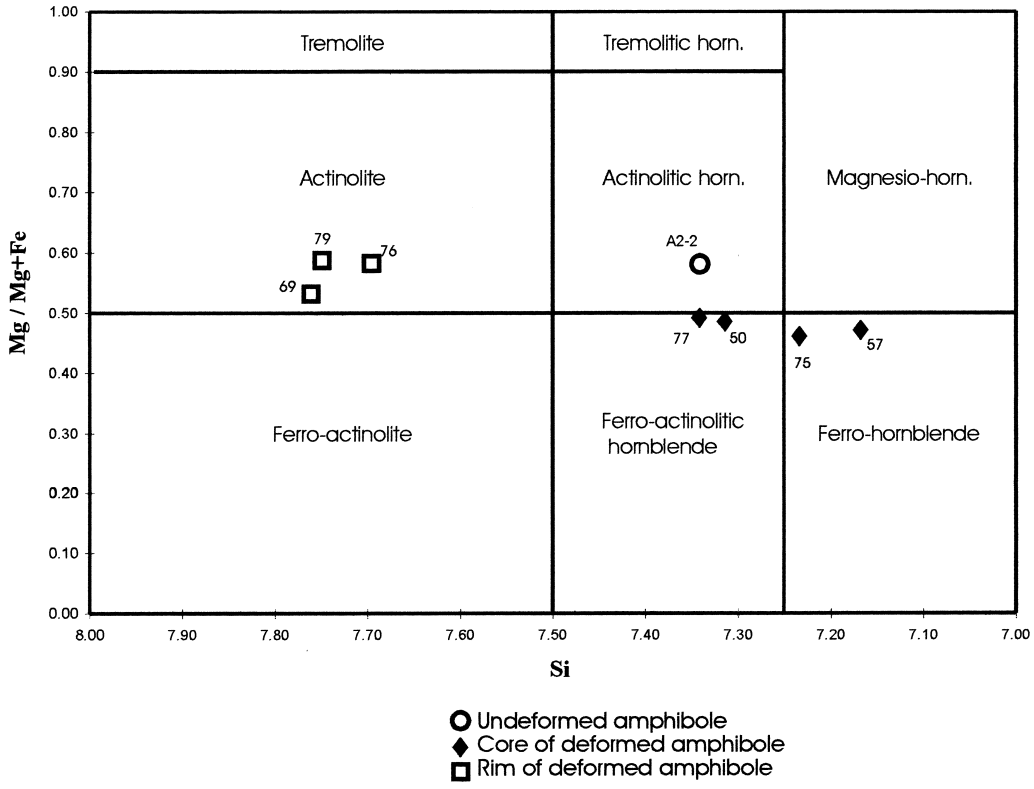

Fig. 8. Position of the undeformed and sheared amphiboles in the international nomenclature (after Leake, 1978).

veins as in the wall rock:

1. Brittle deformation occurred in feldspar and to a lesser extent, in amphibole and allanite. It was responsible for grain-scale cracks then opened and sealed by the deposition of fluid-transported alteration products and additional quartz showing multiple inclusion bands.
2. Alteration-controlled and thus fluid-controlled ductile deformation occurred in biotite, allanite and amphibole.
3. Fluid-enhanced ductile deformation occurred in quartz.
4. Unaltered grains of all species except quartz, were separated one from the other giving rise to intergranular fractures infilled with fluid-transported minerals.
5. Pressure-solution affected most of the minerals and especially their alteration products.

Therefore, vein formation and propagation depend on the deformation mechanisms which can be experienced by the wall rock minerals in the presence of fluids. The absence of deflection or refraction of the rock foliation at the contact with the veins shows that finite shortening was the same in the veins and wall rock and thus, that the veins and the foliation developed contemporaneously. Shear scale veins are composed of aligned grain-scale veins (Fig. 2c) suggesting that they formed from several grain-scale nucleation sites. The sequence of events we suggest for vein development (Fig. 12) is the following: (1) a series of grain-scale cracks (more or less aligned) form; (2) fluids migrate into these cracks; (3) in biotite, alteration occurs as a result of fluid penetration and softens a part of the grain; in feldspars, alteration occurs without softening of the grains and the inter- and intragrain spaces (the future open veins) are infilled with fluid-transported alteration products + additional chlorite and quartz; in quartz, fluids infiltrate grain boundaries which makes surface diffusion flow (Coble creep) easier and, possibly, dislocation creep; (4) ductile deformation affects quartz and altered ferromagnesian minerals while veins develop by widening of intragrain cracks and inter-grain spaces.

The multiple inclusion bands found in quartz in contact with plagioclase show that this sequence of events proceeded as a multi-step process as usual in crack–seal mechanisms.

5. Volume change

In order to investigate composition and volume

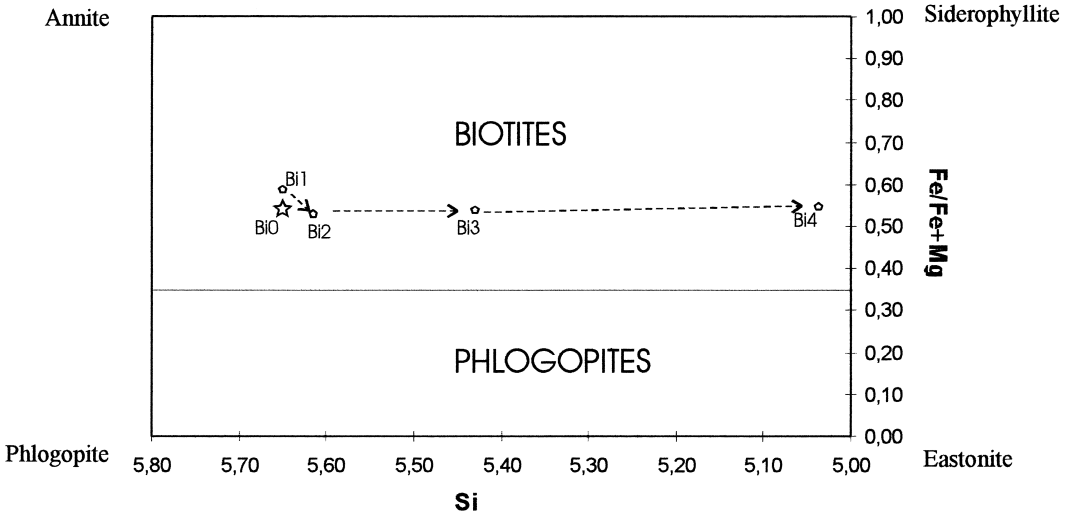

Fig. 9. Position of the phyllites from undeformed granodiorite and from the sheared granodiorite in the phlogopite–biotite composition fields. Bi0: average of five analyses from the undeformed granodiorite. Bi1 is an average of five analyses in the core of a biotite in the sheared granodiorite. Bi2, Bi3, Bi4 are phyllites from the tail of the same biotite grain. Bi1, Bi2, Bi3, Bi4 refer respectively to 1, 2, 3, 4 in Fig. 3(a).

change, four total analyses (major elements and REE) were performed by Chemex Labs Ltd (XRF and ICP–MS methods), one in the undeformed granodiorite of a rhombohedral block limited by conjugate shear zones (N1), one in one of the conjugate shear zones limiting this block (N5), one in two other, highly deformed, shear zones (N9) and one in a shear zone where the deformation is fairly homogeneous and moderate and does not show high-strain bands (N14) (Table 4). Powder has been obtained from the quartering of approximately 1.5 kg of rock in analyses N1, N5 and N9, and of approximately 0.5 kg in analysis N14. In the case of the shear zones, the material was cut along the shear zones boundaries and the remnants of undeformed material hand-removed under binocular-microscope control. The entire width of the shear zone was sampled. Density of the rocks was estimated by means of 3 pycnometer measurements per analysed material. The density of the undeformed granodiorite was also calculated using the modal composition and the densities of rock forming minerals. Average densities were 2750 kg m^{-3} for the undeformed granodiorite (N1), 2790 kg m^{-3} for the moderately sheared material (N14) and 2850 kg m^{-3} for the highly sheared material (N5 and N9).

The chemical composition of the undeformed granodiorite rhombohedral block (N1), which is very close to the average chemical composition of the granodiorite of the Néouvielle massif (Alibert et al., 1988), was first compared with the chemical composition of the

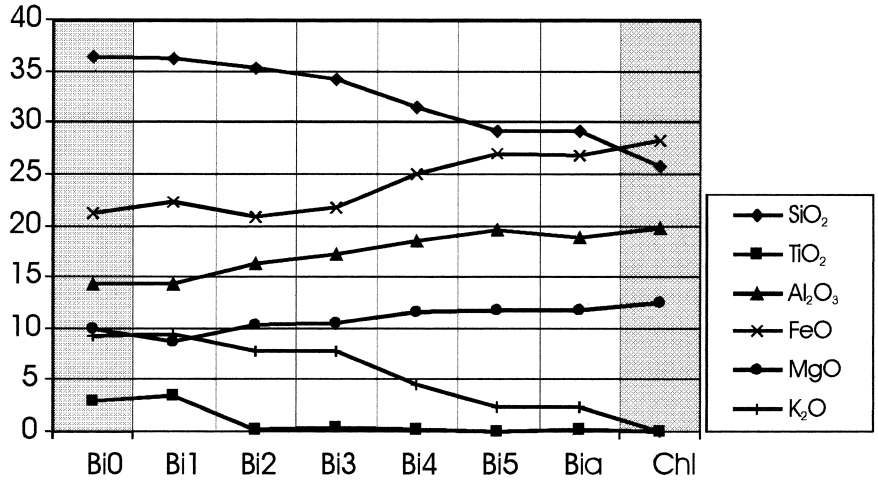

Fig. 10. Evolution of the composition of phyllosilicates in a core-tail structural feature. Bia is an average of four analyses from the tails of four different sheared biotites. Chl is an average of three chlorites formed at the tips of three different biotite grains of the shear zone. Bi1–Bi4 refer respectively to 1–4 in Fig. 3(a). Analyses of Bi0 to Chl phyllites are found in Table 3.

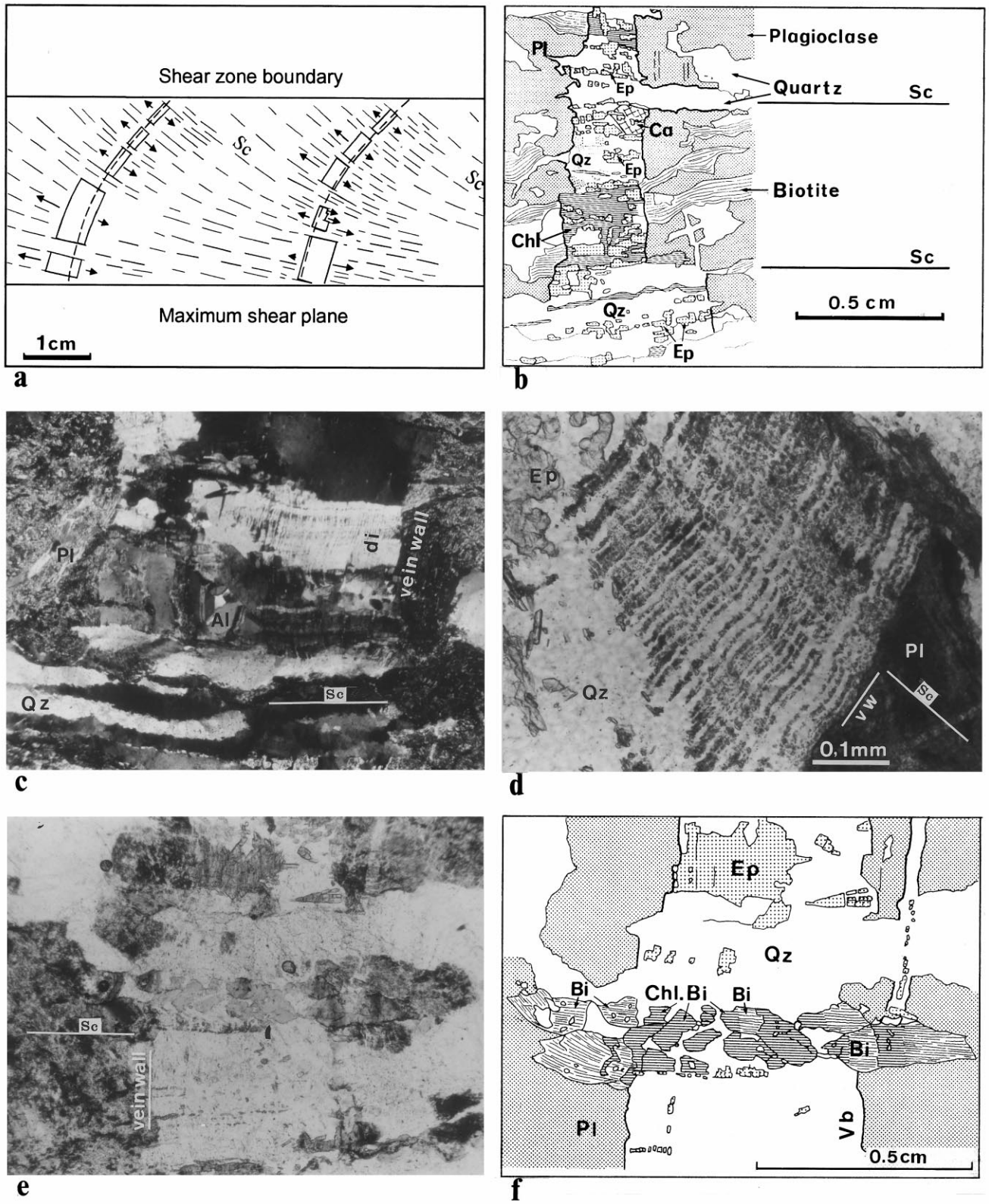

Fig. 11. (a) Development of veins from grain-scale fissures. The fissures opened independently of each other on both sides of a common median line (dashed line) which may give rise to apparent offsets. The length of the arrows is grossly proportional to the distance from the median line on either side. Sc is the major foliation. (b) Transgranular vein filled by quartz (Qz), epidote (Ep), chlorite (Chl), calcite (Ca). On the bottom, the vein is interrupted against an elongate quartz crystal. (c) Transgranular vein with infilling minerals compositionally related to crystals found in the wall rock. Quartz with dark inclusion band (di) developed from plagioclase and albite (Al) from K feldspar. (d) Crack-infilling quartz fibres and epidote (detail). Quartz fibres contain regular inclusion bands which are parallel to the vein wall (vw) and suggest a periodic opening and crack filling (crack–seal mechanism). (e) Crack opening accommodated by biotite alteration and consequent stretching. Plane polarized light. (f) Stretching is concentrated in the chloritized biotite (Chl.Bi) + quartz (Qz) areas formed by alteration of the original biotite which remains unaltered in the crack walls. Note that the boundaries of the 'crack' are diffuse where they traverse the biotite, whereas these boundaries are sharp in the case of the plagioclase crystals.

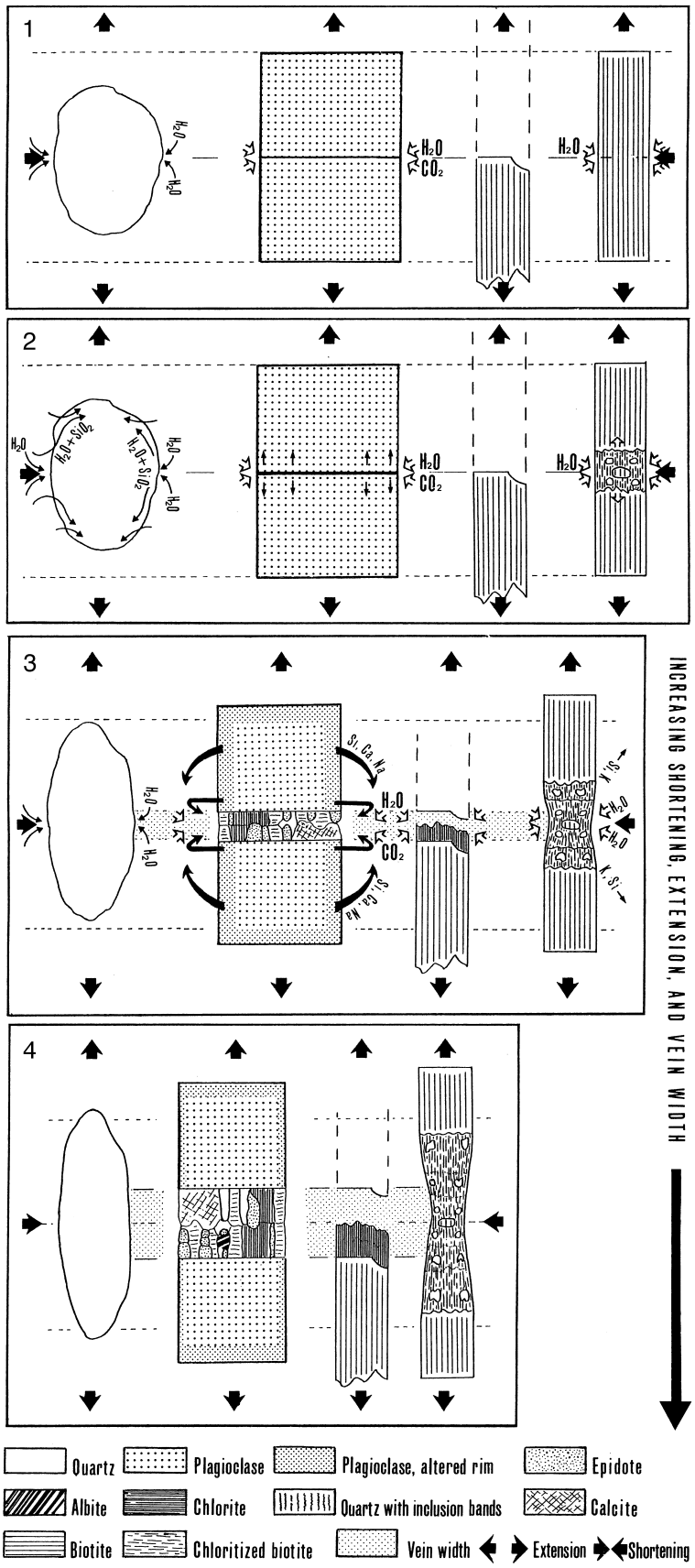

Fig. 12. Schematic model for vein development with increasing strain. 1, 2, 3, and 4 are successive stages of vein development. (1) Grain-scale cracks form in plagioclase and intra-grain scale cracks in biotite; fluids migrate towards these cracks and towards quartz grain boundaries; (2) fluids infiltrate the cracks and the quartz grain boundaries, causing saussuritization of plagioclase, chloritization of biotite and softening of quartz; (3, 4) quartz and chloritized biotite deform by ductile deformation; plagioclase is resolved into two separate blocks with consequent infilling of the crack with albite, quartz, chlorite and calcite, Na, Ca and Si (in part) originating from the solution of the alteration products on the face of the plagioclase perpendicular to the major compressive stress direction; biotite grains separate from adjacent grains giving rise to an intergrain crack and 'pure' chlorite crystallizes in contact with the unaltered biotite.

Table 4
Analyses (major elements and REE) of undeformed and sheared granodiorite. N1: undeformed granodiorite; N5, N9: strongly sheared granodiorite; N14: moderately sheared granodiorite

	Sample	Undeformed rock	Shear zone		
		N1	N5	N9	N14
%	SiO_2	65.68	66.04	64.79	65.33
	TiO_2	0.47	0.44	0.45	0.49
	Al_2O_3	15.53	15.76	15.69	15.73
	Cr_2O_3	0.01	< 0.01	< 0.01	< 0.01
	Fe_2O_3	4.33	4.17	4.24	4.31
	MnO	0.06	0.05	0.05	0.06
	MgO	2.29	1.48	1.46	1.59
	CaO	3.68	4.99	5.09	4.14
	Na_2O	2.86	2.98	2.82	2.29
	K_2O	3.89	2.67	2.86	3.04
	P_2O_5	0.11	0.11	0.12	0.12
	LOI	0.88	1.35	1.66	1.97
	Total	99.79	100.04	99.23	99.07
ppm	Ba	486	540	543	492
	Ce	52	63	64	71
	Dy	4	3.9	4.1	3.9
	Er	1.9	1.8	1.6	1.7
	Eu	1.2	1.6	1.5	1.5
	Gd	3.5	4.3	4.2	4.6
	Ho	0.9	0.8	0.8	0.8
	La	26	34	35	39
	Lu	0.4	0.3	0.3	0.5
	Nd	25	26	25	29
	Pr	5.7	6.5	6.4	7.6
	Sm	5.4	5.6	5.4	5.4
	Tb	0.7	0.6	0.7	0.6
	Tm	0.3	0.4	0.3	0.4
	Yb	2.1	1.5	1.7	1.8
	Rb	161	119	121	124
	Sr	203	280	285	318
	Nb	14	11	14	13
	Zr	129	144	164	162
	Y	23	24	23	25
Densities ($kg\ m^{-3}$)		2750	2850	2850	2790

adjacent shear zones (N5) using Potdevin's treatment (Potdevin, 1993) (Fig. 13) and the mass-balance equation was the following:

$$100\ g\ N1 + 2.42\ g\ SiO_2 + 0.72\ g\ Al_2O_3 + 1.47\ g\ CaO + 0.21\ g\ Na_2O \longrightarrow 97.10\ g\ N5 + 0.03\ g\ Fe_2O_3 + 1.14\ g\ K_2O + 0.76\ g\ MgO$$

with $Fv = 0.995$.

Diagrams (Fig. 13) and mass-balance calculations show that the chemical transformations associated with shear zone development can be considered as isochemical and isovolumetric: (1) variations are quantitatively small and similar to or lower than those reported by several authors in shear zones developed under the same greenschist facies conditions in other areas where the transformations were inferred to have been isochemical and isovolumetric (Beach, 1976; Kerrich et al., 1977; Brodie, 1981; Marquer et al., 1985; Hulsesbosch and Frost, 1989) and by McCaig (1984) in other Pyrenean shear zones (Aston massif); (2) SiO_2 is here immobile whatever the deformation of the rock, whereas SiO_2 shows a high mobility in shear zones where noticeable volume change has occurred (e.g. O'Hara, 1988, 1990; Glazner and Bartley, 1991; Hippertt, 1998); (3) Al_2O_3, TiO_2 and all the REE (Table 4) have identical or very close values in the deformed and undeformed materials. K_2O, CaO and MgO are the only elements showing significant variations.

The chemical composition of the protolith (N1) was then compared to those of a high strain zone (N9) and a moderate strain zone (N14). Mass balance equations are the following:

$$100\ g\ N1 + 1.46\ g\ SiO_2 + 0.73\ g\ Al_2O_3 + 1.19\ g\ CaO + 0.64\ g\ Fe_2O_3 \longrightarrow 99.77\ g\ N9 + 0.93\ g\ K_2O + 0.78\ g\ MgO + 0.06\ g\ Na_2O$$

$$100\ g\ N1 + 0.6\ g\ SiO_2 + 0.4\ g\ Al_2O_3 + 0.12\ g\ CaO + 0.04\ g\ Fe_2O_3 + 0.01\ g\ P_2O_5 \longrightarrow 99.6\ g\ N14 + 0.8\ g\ K_2O + 0.68\ g\ MgO + 0.54\ g\ Na_2O$$

Plots of element (major and REE) concentration in the protolith (N1) vs concentration in the shear zones (N9, N14, N5) (Fig. 14) are in accordance with the trends inferred from the comparison between N1 and N5. Most of the elements (REE and major elements except K_2O and CaO) were immobile. Fe_2O_3 shows an erratic trend with a gain in the transformation N1 → N5 and a loss in the transformation N1 → N9. According to Hippertt (1998) this trend indicates that Fe_2O_3 has probably migrated laterally within the system, rather than been added or removed from it, and thus may be also considered as immobile. MgO shows contents lower in the deformed rocks (1.5%) than in the protolith (2.2%), which could suggest that this element was lost during deformation. This tendency is probably only accidental because the MgO content of the analysed protolith N1 is abnormally high when compared with the usual MgO content of the granodiorite in the Néouvielle massif (0.98–1.55 according to Alibert et al., 1988). K_2O also shows a loss in the shear zones. This tendency, frequently observed in other shear zones developed under greenschist facies conditions (e.g. O'Hara, 1990; Glazner and Bartley, 1991) is ascribed to the chloritization of biotite releas-

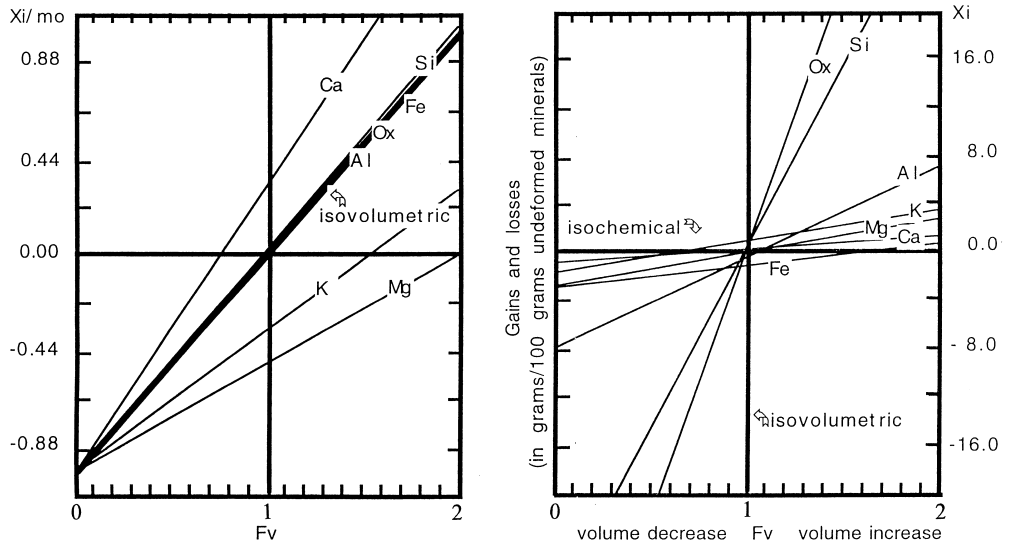

Fig. 13. Composition volume diagrams showing the reaction transforming an undeformed granodiorite (N1) into a highly sheared granodiorite (N5), Potdevin's treatment (Potdevin, 1993) (after Gresens, 1966).

ing K which cannot be fixed where new potash minerals such as microcline are lacking. The gain in CaO is likely to be due to local concentrations in epidote.

Altogether, these shear zones can be thus considered as closed systems.

6. Discussion and conclusion

Although the deformation features may have varied as a function of the behaviour of the mineral species, the observations in the wall rock and vein minerals show that deformation in the shear zone was basically controlled by hydration processes as commonly inferred in similar settings. Among the processes capable of reducing strength, reaction softening (White and Knipe, 1978; Gibson, 1990; Shea and Kronenberg, 1992, 1993; Mares and Kronenberg, 1993; O'Hara, 1994; Hickman et al., 1995; Wintsch et al., 1995) appears to have been effective in biotite, allanite, and, to a lesser extent, amphibole. In plagioclase, which is the most abundant of the granodiorite forming minerals, there was no obvious reaction softening in the usual sense of the word, even though alteration was well developed. It is likely that pressure solution, and especially that of the alteration products, accommodated a noticeable part of finite shortening as shown by the abundance of plagioclase-derived alteration products found in the intra- and inter-grain cracks. In quartz, ductile deformation, although not basically due to fluid effects, is also fluid-enhanced. Softening mechanisms not controlled by fluids such as dynamic recrystallization (Vidal et al., 1980; Knipe, 1989) are limited here to the very high strain bands and can have hardly contributed to shear zone nucleation.

The characteristic common to these mechanisms is that hydration and consequent fluid-controlled alteration and deformation are related to fluid migration towards developing cracks. All these cracks are extensional and formed on the scale of at most a few grains and frequently single grains. The small thickness of these extensional fissures as well as the small total volume they occupy in the shear zones indicate that the volume of circulating fluids was small and dilatancy very low.

In order to interpret the processes of ductile shear zone nucleation we have to consider the fluid origin and the fluid flow mechanisms. Because the shear zones are closed systems, the mobilized fluids are locally derived. Numerous studies have shown that in such a material an ubiquitous fluid is present in a variety of intragranular and intergranular sites (Etheridge, 1983; Kronenberg et al., 1990; Hippertt, 1994) and that fluid pressure P_f is close to lithostatic pressure during greenschist facies metamorphism (Etheridge et al., 1984; Sibson, 1992; Ridley, 1993; Ferry, 1994).

The fluid pressure P_f at a depth z, in a rock mass of average density ρ is conveniently defined, in relation to the overburden pressure $\sigma_v = \rho g z$ where g is the gravitational acceleration, by means of the pore pressure factor $\lambda = P_f/\sigma_v$. The value of the rock presure σ_v may vary between those of the principal compressive stresses according to the tectonic environment; σ_v will only be equal to the mean stress $\sigma_m = (\sigma_1 + \sigma_2 + \sigma_3)/3$ in the restricted circumstances that the rock is behaving as a fluid, i.e. $\sigma_1 = \sigma_2 = \sigma_3$, or that $\sigma_v = \sigma_2$ and

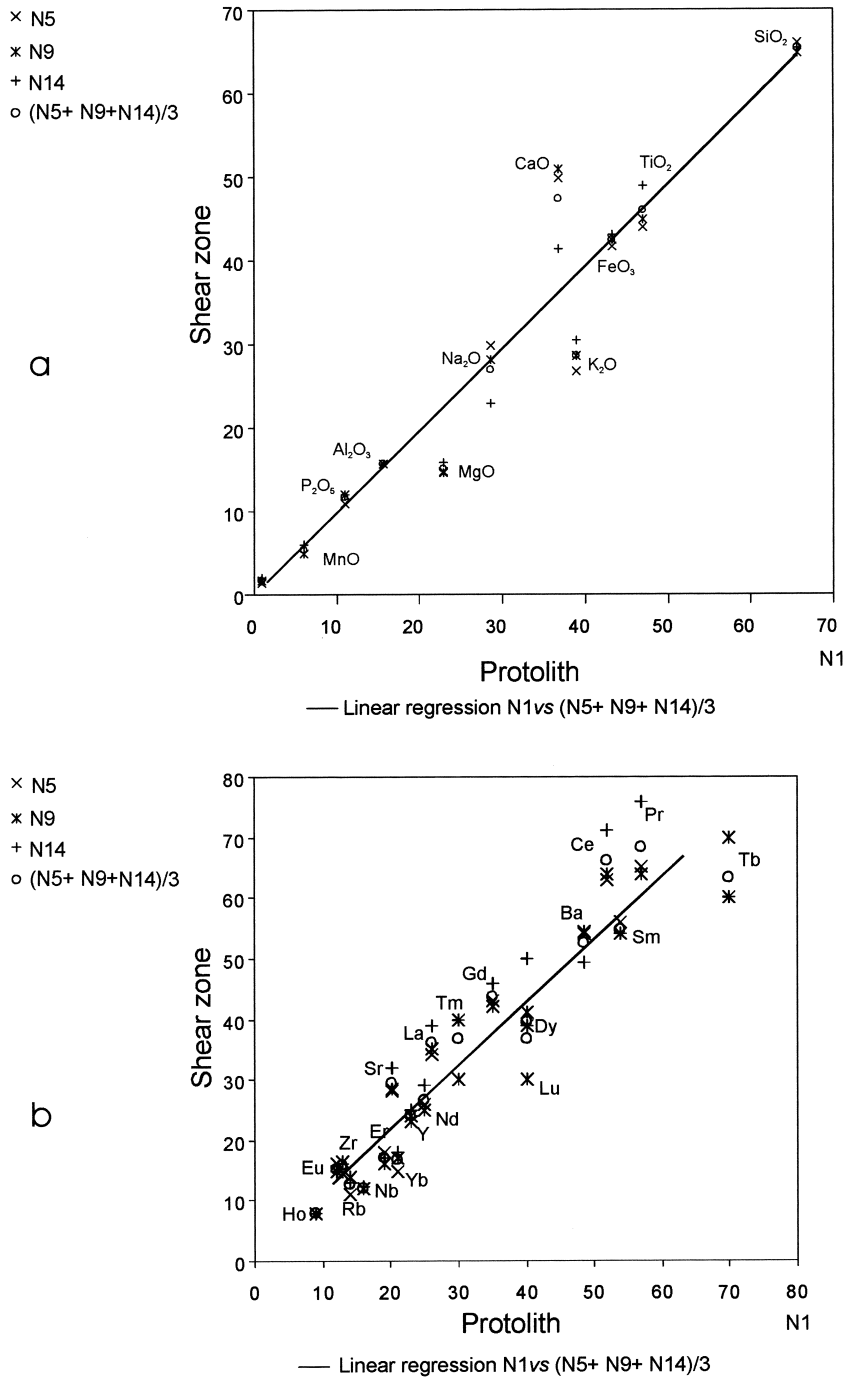

Fig. 14. Plots of element concentrations in the protolith (N1) vs concentration in the analysed shear zones referred to as N5, N9, N14 (see text and Table 4) and the average (N5 + N9 + N14)/3 (values multiplied by scaling factors). (a) Major elements. (b) REE.

$\sigma_v = (\sigma_1 + \sigma_3)/2$. If controlled by rock pressure, fluid pressure is described as lithostatic and $\lambda = 1$.

The extensional nature of microfractures observed (Figs. 2c, 3c, d, 11c–f and 12) is indicative of high pore fluid pressures greater than the minimum compressive stress σ_3 during the nucleation of the studied shear zones. The fluid flow mechanism is interpreted as resulting from the heterogeneous character of the material.

Effectively, on the scale of the outcrops (1 m) the undeformed granodiorite is an homogeneous polymineralic rock, but on the scale of the shear zone (a

few cm) it is a mechanically highly heterogeneous rock made up of different solid phases with different shapes and different rheological behaviour and strength.

Spatial variations in mean stresses are expected in a stress field acting on a rheologically heterogeneous rock. Stress field geometries are scale-independent and reflect the scale of inhomogeneity in the rock (Ridley, 1993). Models showing stress distribution around strong inclusions in a weaker medium indicate that a strong body tends to act as a stress guide (Oliver et al., 1990): within the stronger body and in a specific area around it, both the orientation and magnitude of mean and differential stress change relative to the far-field deviatoric stress (Edwards, 1951; Eshelby, 1957; Strömgard, 1973; Jaeger and Cook, 1979).

The natural grain-scale stress field in a polymineralic rock with elements of high contrasting rheology, such as the Néouvielle granodiorite, is much more complex than the theoretical stress fields in the models. Furthermore, areas of strain incompatibility must arise because of the high content of strong minerals (Debat et al., 1978; Oliver et al., 1990).

At least two related processes may have been important in controlling grain-scale fluid flow:

1. As fluid pressures are buffered close to the lithostatic value ($\lambda \approx 1$) then variation in fluid pressure P_f will mimic variations in mean stress σ_m. A spatial gradient in fluid pressure will thus be maintained by local mean stress variations and there will be a tendency for fluid to flow towards the low mean stress zones, i.e. the relatively low fluid pressure zones. This results in local increase in P_f and may give rise to tensile crack growth by hydraulic fracturing.
2. Zones of low mean and differential stresses constitute perfect regions of tensile failure, microfracturing and attendant dilatancy. According to Oliver et al. (1990), in zones where both mean and differential stresses are low, tensile failure may occur at relatively low fluid pressure, whereas in zones where all stresses are high, high fluid pressure does not result in failure, even though fluid pressure is substantially higher than in the low mean stress zones (Fig. 8, Oliver et al., 1990); tensile failure by hydraulic fracturing requires that fluid pressure P_f exceeds the minimum principal stress σ_3 by at least the tensile strength of the rock T_0, $P_f = \sigma_3 + T_0$ and that the differential stress is sufficiently low to inhibit shear failure, $(\sigma_1 - \sigma_3) < 4T_0$. This process will be efficient provided that the stress heterogeneity of the rock is sufficiently large.

The opening of microcracks lowers the fluid pressure locally and produces local fluid pressure gradients to drive fluid migration. These grain-scale mechanisms are favourable not only for localizing brittle deformation but also for focusing locally derived fluids; short distance fluid migration to dilatant sites takes place.

Hydration and consequent fluid controlled alteration of minerals promote local softening processes such as reaction enhanced ductility and hydraulic weakening. Each stage of grain fracturing creates a new surface area on which chemical reaction can start to produce a more ductile matrix. Reduction in yield strength is responsible for ductile strain nucleation: these localities become preferential sites for further deformation to be concentrated. When the quantity of hard minerals softened reaches a critical point the deformation spreads out into surrounding areas; the shear deformation progressively localizes along the so formed weak sites and the shear zone nucleates.

In the proposed mechanism the distribution of possible sites of ductile strain nucleation is connected with the distribution of heterogeneities in the undeformed rock, i.e. is connected with the distribution of mineral species. The homogeneous distribution of these sites leads to patterns of diffuse deformation. On the scale of a single shear zone, this explains why there are multiple very high strain bands (which may represent the initial location of the early initiation sites). At outcrop scale this explains why there is the development of networks of numerous conjugate, fairly parallel and regularly spaced small-scale shear zones.

Water stored in granodiorite undergoing retrogression is likely to be rapidly consumed by hydration reactions: processes of local softening are progressively discontinued and consequently the shear zone propagation into previously unperturbed region is interrupted. The fact that the shear zones develop as chemically closed systems in addition to the relatively small volume of fluids available in the granodiorite may explain why the deformation does not localize severely into a small number of discrete shear zones.

The mechanisms suggested for the nucleation and propagation of the small-scale brittle–ductile shear zones observed in the Néouvielle massif are consistent with the concept of premonitary shear zones (Johnson, 1995); according to Johnson the formation of shear zones, that may precede the formation of faults, is essentially evolutionary: 'failure occurs in stages and each stage the rock is changed permanently into a different material' (Johnson, 1995, p. 160). Clearly, in our mechanism, the processes involving fluids stored in the rock, initiated on pre-existing heterogeneities (rheologically heterogeneous polymineralic granodiorite) and then the deformation nucleated and propagated on subsequent induced heterogeneities (progressive changes in mineral composition and microstructures). Even though fluids are involved, the fundamental process is thus the propagation of instabilities as suggested by Cobbold (1977). The deformation stopped after the

small brittle–ductile shear zones formed because of draining and drying of the rock and the structures are simply small-scale shear zones. In other situations where the processes of deformation continue, for instance because of large influx of fluids from elsewhere, the small-scale shear zones may evolve into regional shear zones or faults.

Acknowledgements

We thank K.D. O'Hara, A. McCaig and T.G. Blenkinsop for their constructive criticism and suggestions. D. Debat performed the mass-balance calculations.

References

Alibert, Ch., Debon, F., Ternet, Y., 1988. Le pluton à structure concentrique du Néouvielle (Hautes Pyrénées): typologie chimique, âge et genèse. Comptes Rendus de l'Académie des Sciences Paris 306, 49–54.

Allison, I., La Tour, T.E., 1977. Brittle deformation of hornblende in a mylonite: a direct geometrical analogue of ductile deformation by translation gliding. Canadian Journal of Earth Sciences 14, 1953–1958.

Babaie, H.A., La Tour, T.E., 1994. Semibrittle and cataclastic deformation of hornblende–quartz rocks in a ductile shear zone. Tectonophysics 229, 19–30.

Beach, A., 1976. The interrelations of fluid transport, deformation, geochemistry and heat flow in early Proterozoic shear zones in the Lewissian complex. Philosophical Transactions of the Royal Society of London A280, 569–604.

Bell, T.H., Etheridge, M.M., 1976. The deformation and recrystallization of quartz in a mylonite zone, Central Australia. Tectonophysics 32, 235–268.

Berthé, D., Choukroune, P., Jegouzo, P., 1979. Orthogneiss, mylonite and non-coaxial deformation of granite: the example of the South Armorican shear zone. Journal of Structural Geology 1, 30–42.

Blacic, J.D., Christie, J.M., 1984. Plasticity and hydrolytic weakening of quartz single crystals. Journal of Geophysical Research 89, 4223–4239.

Brodie, K.H., 1981. Variation in Amphibole and Plagioclase composition with deformation. Tectonophysics 78, 385–402.

Cobbold, P.R., 1977. Description and origin of banded deformation structures. I Regional strain, local perturbations and deformation bands. Canadian Journal of Earth Sciences 14, 1721–1731.

Coble, R.L., 1963. A model for boundary diffusion controlled creep in polycrystalline material. Journal of Applied Physics 34, 1979–1982.

Cox, S.F., Etheridge, M.A., 1989. Coupled grain-scale dilatancy and mass transfer during deformation at high fluid pressures: examples from Mount Lyell, Tasmania. Journal of Structural Geology 11, 147–162.

Debat, P., Sirieys, P., Déramond, J., Soula, J.C., 1975. Paléodéformation d'un massif orthogneissique. Tectonophysics 28, 159–183.

Debat, P., Soula, J.C., Kubin, L., Vidal, J.L., 1978. Optical studies of natural deformation microstructures in feldspars (gneiss and pegmatites from Occitania, southern France). Lithos 11, 133–145.

Edwards, R.H., 1951. Stress concentration around spheroidal inclusions and cavities. Journal of Applied Mechanics 18, 19–30.

Elliott, D., 1972. Deformation paths in Structural Geology. Geological Society of America Bulletin 83, 2621–2638.

Eshelby, M.A., 1957. The determination of the elastic field of an ellipsoidal inclusion, and related problems. Proceedings of the Royal Society of London 1241, 376–396.

Etheridge, M.A., 1983. Differential stress magnitudes during regional deformation and metamorphism: upper bound imposed by tensile fracturing. Geology 11, 231–234.

Etheridge, M.A., Wall, V.J., Cox, S.F., Vernon, R.H., 1984. High fluid pressures during regional metamorphism and deformation: implications for mass transport and deformation mechanisms. Journal of Geophysical Research 89, 4344–4558.

Ferry, J.M., 1994. A historical review of metamorphic fluid flow. Journal of Geophysical Research 99, 15487–15498.

Gay, N.C., 1968. Pure shear and simple deformation of inhomogeneous viscous fluids, I: Theory. Tectonophysics 5, 211–234.

Gibson, R.G., 1990. Nucleation and growth of retrograde shear zones: an example from the Needle Mountains, Colorado, USA. Journal of Geology 102, 331–348.

Glazner, A.F., Bartley, J.M., 1991. Volume loss fluid flow and state of strain in extensional mylonites from the central Mojave Desert, California. Journal of Structural Geology 13, 587–594.

Gresens, R.L., 1966. Composition–volume relations of metasomatism. Chemical Geology 2, 47–65.

Griggs, D.T., 1974. A model of hydrolytic weakening in quartz. Journal of Geophysical Research 79, 1653–1661.

Griggs, D.T., Blacic, J.D., 1964. The strength of quartz in the ductile regime (abstract). EOS Transactions of the American Geophysical Union 45, 102–103.

Griggs, D.T., Blacic, J.D., 1965. Quartz: anomalous weakening of synthetic crystals. Science 147, 292–295.

Handy, M.R., 1990. The solid-state flow of polymineralic rocks. Journal of Geophysical Research 95, 8647–8661.

Handy, M.R., 1994. Flow laws for rocks containing two non-linear viscous phases: a phenomenological approach. Journal of Structural Geology 16, 287–301.

Henderson, I.H.C., McCaig, A.M., 1996. Fluid pressure and salinity in shear zone-related veins, central Pyrenees, France: Implications for the fault-valve model. Tectonophysics 262, 321–348.

Hickman, S.H., Sibson, R., Bruhn, R., 1995. Introduction to special section mechanical involvement of fluids in faulting. Journal of Geophysical Research 100, 12831–12840.

Hippertt, J.F., 1994. Strain boundary microstructures in micaceous quartzite: significance for fluid movement and deformation processes in low metamorphic grade shear zones. Journal of Geology 102, 331–348.

Hippertt, J.F., 1998. Breakdown of feldspar, volume gain and lateral mass transfer during mylonitization of granitoid in a low metamorphic grade shear zone. Journal of Structural Geology 20, 175–193.

Hobbs, B.E., 1968. Recrystallization of single crystals of quartz. Tectonophysics 6, 353–401.

Hulsesbosch, T.P., Frost, B.R., 1989. Mineral changes, element mobility, and fluids associated with deep shearing in the Mount Helen structural belt, Wyoming, U.S.A. In: Bridgwater, D (Ed.), Fluid Movements—Element Transport and the Composition of the Deep Crust. Kluwer Academic, Dordrecht, pp. 139–150.

Jaeger, J.C., Cook, N.G.W., 1979. Fundamentals of Rock Mechanics, 3rd ed. Chapman & Hall, London 593 pp.

Johnson, A.M., 1995. Orientations of faults determined by premonitary shear zones. Tectonophysics 247, 161–238.

Kamineni, D.C., Thiviege, R.H., Stone, D., 1988. Development of a cataclastic fault zone in an Archean granitic pluton of the Superior Province: structural, geochemical and geophysical characteristics. American Journal of Science 288, 458–494.

Kerrich, R., 1986. Fluid transport in lineaments. Philosophical Transactions of the Royal Society of London A317, 219–251.

Kerrich, R., Fyfe, W.S., Gorman, B.E., Allison, I., 1977. Local modification of rock chemistry by deformation. Contributions in Mineralogy and Petrology 65, 183–190.

Kerrich, R., Allison, I., Barnett, R.L., Moss, S., Starkey, J., 1980. Microstructural and chemical accompanying deformation of granite in a shear zone at Miéville, Switzerland; With implications for stress corrosion cracking and superplastic flow. Contributions in Mineralogy and Petrology 73, 221–241.

Kirby, S.H., 1984. Chemical effects of water on rock deformation. Journal of Geophysical Research 89, 3991–3995.

Kirby, S.H., Kronenberg, A.K., 1984. Hydrolytic weakening of quartz: Uptake of molecular water and the role of microfracturing (abs). EOS Transactions of the American Geophysical Union 65, 277.

Knipe, R.J., 1989. Deformation mechanisms—recognition from natural tectonites. Journal of Structural Geology 11, 127–146.

Kronenberg, A.K., Segall, P., Wolf, G.H., 1990. Hydrolitic weakening and penetrative deformation within a natural shear zone. In: Geophysical Monograph, 56. American Geophysical Union, Washington, pp. 21–36.

Lamouroux, C., 1976. Les mylonites dans le massif du Néouvielle (textures, déformations intracristallines). Déformations pyrénéennes dans un complexe plutonique hercynien. Thèse 3° cycle Toulouse, 137 pp.

Lamouroux, C., 1987. Les Mylonites des Pyrénées—Classification, mode de formation, évolution. Société Géologique du Nord 19, 373 pp.

Lamouroux, C., Debat, P., Déramond, J., Majesté-Menjoulas, C., 1979. Influence de massifs plutoniques hercyniens sur l'évolution des structures pyrénéenne: exemple du massif de Néouvielle. Bulletin de la Société Géologique de France 7 (XXI), 201–211.

Lamouroux, C., Soula, J.C., Déramond, J., Debat, P., 1980. Shear zones in the granodioritic massifs of the Central Pyrenees and the behaviour of these massifs during Alpine orogenesis. Journal of Structural Geology 2, 49–53.

Lamouroux, C., Soula, J.C., Roddaz, B., 1981. Les zones mylonitiques des massifs du Bassiès et de l'Aston (Haute Ariège). Bulletin du B.R.G.M. 1, 103–111.

Lamouroux, C., Ingles, J., Debat, P., 1991. Conjugate ductile shear zones. Tectonophysics 185, 309–323.

Lamouroux, C., Debat, P., Ingles, J., Guerrero, N., Sirieys, P., Soula, J.C., 1994. Rheological properties of rocks inferred from the geometry and microstructures in two natural shear zones. Mechanics of Materials 18, 79–87.

Leake, B.E., 1978. Nomenclature of amphiboles. Mineralogical Magazine 42, 533–563.

Losh, S., 1989. Fluid–rock interaction in an evolving ductile shear zone and across the brittle–ductile transition, Central Pyrenees, France. American Journal of Science 278, 600–648.

Mares, V.M., Kronenberg, A.K., 1993. Experimental deformation of muscovite. Journal of Structural Geology 15, 1061–1075.

Marquer, D., Gapais, D., Capdevila, R., 1985. Comportement chimique et orthogneissification d'une granodiorite en faciès schistes verts (Massif de l'Aar, Alpes centrales). Bulletin de Minéralogie 108, 209–221.

McCaig, A., 1984. Fluid–rock interaction in some shear zones from the Pyrenees. Journal of Metamorphic Geology 2, 129–142.

Mitra, G., 1978. Ductile deformation zones and mylonites: the mechanical processes involved in the deformation of crystalline basement. American Journal of Science 278, 1057–1084.

Nutman, A.P., Rivers, T., Longstaffe, F., Park, J.F.W., 1989. The Ataneq fault and mid-proterozoic retrograde metamorphism of early Archean tonalites of the Isukasia area, southern west Greenland: reaction, fluid composition and implications for regional studies. In: Bridgwater, D (Ed.), Fluid Movements—Element Transport and the Composition of the Deep Crust. Kluwer Academic, Dordrecht, pp. 151–170.

O'Hara, K.D., 1988. Fluid flow and volume loss during mylonitization: an origin for phyllonite in an overthrust setting, North Carolina, USA. Tectonophysics 156, 21–36.

O'Hara, K.D., 1990. State of strain in mylonites from the western Blue Ridge province, southern Appalachians: the role of volume loss. Journal of Structural Geology 12, 419–431.

O'Hara, K.D., 1994. Fluid interaction in crustal shear zones: A directed percolation approach. Geology 22, 843–846.

Oliver, N.H.S., Valenta, R.K., Wall, V.J., 1990. The effect of heterogeneous stress and strain on metamorphic fluid flow, Mary Kathleen, Australia, and a model for large-scale fluid circulation. Journal of Metamorphic Geology 8, 311–331.

Parseval (de), Ph., 1992. Étude minéralogique et géochimique du gisement de talc de Trimouns. Thèse Université Paul Sabatier, Toulouse III, 227 pp.

Poirier, J.P., 1980. Shear localization and shear instability in materials in the ductile field. Journal of Structural Geology 2, 135–142.

Potdevin, J.L., 1993. Gresens 92: Simple MacIntosh program of the Gresens method. Computers and Geosciences 19, 1229–1238.

Pouget, P., Lamouroux, C., Dahmani, A., Debat, P., Driouch, Y., Mercier, A., Soula, J.C., Vézat, R., 1989. Typologie et mise en place des roches magmatiques dans les Pyrénées hercyniennes. Geologische Rundschau 78, 537–554.

Raleigh, C.B., Paterson, M.S., 1965. Experimental deformation of serpentinite and its tectonic implications. Journal of Geophysical Research 70, 3965–3985.

Ramsay, J.G., Graham, R.H., 1970. Strain variations in shear belts. Canadian Journal of Earth Sciences 7, 796–823.

Ramsay, J.G., Huber, M., 1987. In: The Techniques of Modern Structural Geology, Volume 2: Folds and Fractures. Academic Press, London.

Ridley, J., 1993. The relations between mean rock stress and fluid flow in the crust: with reference to vein- and lode-style gold deposits. Ore Geology Reviews 16, 419–429.

Rudnicki, J.W., 1977. The inception of faulting in a rock mass with a weakened zone. Journal of Geophysical Research 82, 844–854.

Segall, P., Pollard, D.D., 1983. Joint formation in the granitic rock of the Sierra Nevada. Geological Society of America Bulletin 94, 563–575.

Segall, P., Simpson, C., 1986. Nucleation of ductile shear zones on dilatant fractures. Geology 14, 56–59.

Shea, W.T., Kronenberg, A.K., 1992. Rheology and deformation mechanisms of an isotropic mica schist. Journal of Geophysical Research 97, 15201–15237.

Shea, W.T., Kronenberg, A.K., 1993. Strength and anisotropy of foliated rocks with varied mica contents. Journal of Structural Geology 15, 1097–1121.

Sibson, R.H., 1992. Implications of fault valve behaviour for rupture nucleation and recurrence. Tectonophysics 211, 283–293.

Soula, J.C., Lamouroux, C., Viallard, P., Bessiere, G., Debat, P., Ferret, B., 1986. The mylonite zones in the Pyrenees and their place in the Alpine tectonic evolution. Tectonophysics 129, 115–147.

Strömgard, K.E., 1973. Stress distribution during formation of boudinage and pressure shadows. Tectonophysics 16, 215–248.

Takagi, H., 1989. Ductile shear zones: microstructures of mylonites. In: Karato, S.I, Torium, M (Eds.), Rheology of Solids and of the Earth, vol. 54. Oxford Science, Oxford, pp. 338–350.

Tourigny, G., Tremblay, A., 1997. Origin and incremental evolution of brittle/ductile shear zones in granitic rocks: natural examples from the southern Abitibi belt, Canada. Journal of Structural Geology 19, 15–27.

Tullis, J., Yund, R., Farver, J., 1996. Deformation-enhanced fluid

distribution in feldspar aggregates and implications for ductile shear zones. Geology 24, 63–66.

Vidal, J.L., Kubin, L., Debat, P., Soula, J.C., 1980. Deformation and dynamic recrystallization of K feldspar augen in orthogneiss from Montagne Noire, Occitania, Southern France. Lithos 13, 247–255.

Wayne, D.M., McCaig, A.M., 1998. Dating fluid flow in shear zones: Rb–Sr and U–Pb studies of syntectonic veins in the Néouvielle Massif, Pyrenees. In: Parnell, J (Ed.), Dating and Duration of Fluid Flow and Fluid–Rock Interaction, Geological Society of London Special Publication, 144, pp. 129–136.

White, S.H., 1977. Geological significance of recovery and recrystallization processes in quartz. Tectonophysics 39, 143–170.

White, S.H., Knipe, R.J., 1978. Transformation- and reaction-enhanced ductility in rocks. Journal of the Geological Society of London 135, 513–516.

White, S.H., Burrows, S.E., Carreras, J., Shaw, N.D., Humphreys, F.J., 1980. On mylonites in ductile shear zones. Journal of Structural Geology 2, 175–187.

Wintsch, R.P., Christoffensen, R., Kronenberg, A.K., 1995. Fluid–rock reaction weakening of fault zones. Journal of Geophysical Research 100, 13021–13032.